

Three Dimensional Boundary Layer Flow over Unsteady Continuous Moving Surface Embedded in a Nanofluid

Mohamed S. Abdel-wahed^{*1}, Mohamed Y. AKL²

¹Basic sciences Department, Faculty of Engineering at benha, Benha University, Cairo, Egypt

²Engineering Mathematics and Physics Department, Faculty of Engineering at shoubra, Benha University, Cairo, Egypt

*¹eng_moh_sayed@live.com

Abstract

The effects of nanoparticles type, Nanoparticles concentration (volume fraction), unsteadiness parameter and stretching parameter on the mechanical properties of unsteady moving surface embedded into cooling medium consists of water with Cu or Ag or Al₂O₃ particles are studied. The governing time dependent boundary layer equations are transformed to ordinary differential equations containing stretching parameter, unsteadiness parameter, nanoparticle volume fraction and Prandtl number. These equations are solved numerically. The velocity and temperature profiles of the boundary layer are plotted and discussed in details for various values of the different parameters

Keywords

Nanofluid; Heat Transfer; Suction Injection; Three Dimensional Boundary Layer; Mechanical Properties

Introduction

In the last few years, the nanofluids have been suggested as a new cooling medium Because they have novel properties that make them potentially useful in many applications in heat transfer including microelectronics, fuel cells, engine cooling/vehicle thermal management, chiller, heat exchanger, nuclear reactor coolant, grinding, machining, space technology, defense and ships, and boiler flue gas temperature reduction.

Choi [1] was the first one introduce the term of "Nanofluid" that represents the fluid in which Nano-scale particles are suspended in the base fluid with low thermal conductivity such as water, ethylene glycol, oils, etc. The impact of the nanofluids on the boundary layer behavior over a moving surface during the cooling stage has been analyzed by a lot of researchers. Yacob et al. [2] studied the boundary layer flow past a stretching/shrinkage surface beneath an external uniform shear flow in nanofluids. Aminreze et al. [3] investigated the effect of partial slip boundary condition on the flow and heat transfer of Nanofluid past stretching sheet prescribed constant wall temperature. Rana et al. [4] introduce the flow and heat transfer of a Nanofluid over a nonlinearly stretching sheet. Alsaedi et al. [5] studied the effects of heat generation/absorption on stagnation point flow of Nanofluid over a surface with convective boundary conditions. Hamad [6] deduced an analytical solution of natural convection flow of Nanofluid over a linearly stretching sheet in the presence of magnetic field. Aziz et al. [7] introduced the Natural convective boundary layer flow of a Nanofluid past a convectively heated vertical plate. Fang et al. [8] studied the boundary layer flow over a stretching sheet with variable thickness. Elbashbeshy et al. [9] Deduced an exact solution of boundary layer flow over a moving surface embedded into a Nanofluid in the presence of magnetic field and suction/injection. Elbashbeshy et al. [10] investigated the effect of magnetic field on flow and heat transfer of a Nanofluid over an unsteady continuous moving surface in the presence of suction/injection. Elbashbeshy et al. [11] studied the effect non-linear velocity and variable thickness on the Nanofluid boundary layer in the presence of thermal radiation. Elbashbeshy et al. [12] studied the effect of thermal radiation and heat generation on the mechanical properties of unsteady continuous moving cylinder in a Nanofluid in the presence of suction or

injection. Elbashbeshy et al. [13] studied the Effect of heat treatment process with a new cooling medium (Nanofluid) on the mechanical properties of an unsteady continuous moving cylinder.

Three dimensional flow problem of a regular fluid has been discussed by Nazar et. al. [14] investigated the effects of viscoelastic fluid on the velocity profiles of three dimensional flows over a stretching surface. Takhar et. al. [15] studied the effects of heat transfer on three dimensional MHD boundary layer flow through a stretching surface. El-dabe et. al. [16] studied the effects of heat generation/absorption and chemical reaction on three dimensional viscoelastic fluids through a stretching surface. Aboeldahab et. al. [17] studied the combined free convective heat and mass transfer effects on the unsteady three-dimensional laminar flow over a time dependent stretching surface. Elbashbeshy et al. [18] study the effects of the thermal radiation, heat generation and first order chemical reaction on heat and mass transfer on a steady three dimensional flow over stretching surface. Gireesha et al. [19] examined the thermal radiation and hall current effect on the boundary layer flow over non-isothermal stretching surface. Mahanthesh et al. [20] investigated theoretically the hydromagnetic three-dimensional boundary layer flow of nanofluid due to stretching sheet in the presence of a non-linear thermal radiation as well as Soret and Dufour effects.

Mahanthesh et al. [21] present a numerical study to three-dimensional electrically conducting flow over a non-linear stretching surface under the influence of thermal radiation, Joule heating and viscous dissipation.

This paper presents a mathematical model of the cooling stage of three dimensional plate using Nanofluid as a new cooling medium. The impact of the coolant on the boundary layer behavior and mechanical properties of the surface are considered.

Problem Formulation

Consider an unsteady, laminar, and incompressible Nanofluid on a continuous moving surface. The fluid is water based Nanofluid containing three types of nanoparticles, either Cu (Copper) or Ag (Silver) or Al₂O₃ (Aluminum oxide). The nanoparticles are assumed to have a uniform shape and size. Moreover, it is assumed that both the fluid phase and nanoparticles are in thermal equilibrium state. As shown in fig. (1) The x, y-axes are run through the surface and the z-axis is perpendicular to it.

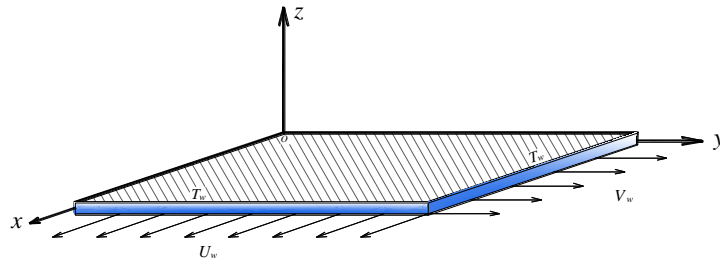


FIGURE (1) PHYSICAL MODEL AND COORDINATE SYSTEM

2.1 The Conservation Equations for the Unsteady Boundary Layer

$$\frac{\partial u}{\partial x} + \frac{\partial v}{\partial y} + \frac{\partial w}{\partial z} = 0 \quad (1)$$

$$\frac{\partial u}{\partial t} + u \frac{\partial u}{\partial x} + v \frac{\partial u}{\partial y} + w \frac{\partial u}{\partial z} = \left(\frac{\mu_{nf}}{\rho_{nf}} \right) \frac{\partial^2 u}{\partial z^2} \quad (2)$$

$$\frac{\partial v}{\partial t} + u \frac{\partial v}{\partial x} + v \frac{\partial v}{\partial y} + w \frac{\partial v}{\partial z} = \left(\frac{\mu_{nf}}{\rho_{nf}} \right) \frac{\partial^2 v}{\partial z^2} \quad (3)$$

$$\frac{\partial T}{\partial t} + u \frac{\partial T}{\partial x} + v \frac{\partial T}{\partial y} + w \frac{\partial T}{\partial z} = \alpha_{nf} \frac{\partial^2 T}{\partial z^2} \quad (4)$$

Subjected to the boundary conditions

$$\begin{aligned} u = U_w, \quad v = V_w, \quad T = T_w, \quad \text{at } z = 0 \\ u = 0, \quad v = 0, w = 0, \quad T = T_\infty, \quad \frac{\partial u}{\partial z} = \frac{\partial v}{\partial z} = 0 \quad \text{as } z \rightarrow \infty \end{aligned} \quad (5)$$

Where u, v and w are velocity components in the x, y and z directions, respectively, t is the time, μ_{nf} is the nanofluid dynamic viscosity, ρ_{nf} is the density of the nanofluid, T is the temperature of the nanofluid, α_{nf} is the thermal diffusion of the nanofluid.

It is assumed that the velocity of the surface along x and y axes respectively are U_w and V_w , also the surface temperature is T_w .

$$\left. \begin{aligned} U_w(x, t) = \frac{ax}{(1-\gamma)}, \quad V_w(y, t) = \frac{by}{(1-\gamma)}, \\ T_w(x, y, t) = T_\infty + \frac{c_1 x}{(1-\gamma)} = T_\infty + \frac{c_2 y}{(1-\gamma)} \end{aligned} \right\} \quad (6)$$

Where a, b, c_1, c_2 and γ are positive constants with ($\gamma t < 1$). The properties of Nanofluid are defined as follows (see [16]).

$$\begin{aligned} \mu_{nf} = \frac{\mu_f}{(1-\phi)^{2.5}}, \quad \rho_{nf} = (1-\phi)\rho_f + \phi\rho_s, \quad \alpha_{nf} = \frac{k_{nf}}{(\rho C_p)_{nf}} \\ (\rho C_p)_{nf} = (1-\phi)(\rho C_p)_f + \phi(\rho C_p)_s, \quad \frac{k_{nf}}{k_f} = \frac{(k_s + 2k_f) - 2\phi(k_f - k_s)}{(k_s + 2k_f) + \phi(k_f - k_s)} \end{aligned}$$

where ϕ is Nanoparticles volume fraction, it is worth mentioning that the study reduces to those of a viscous or regular fluid when ($\phi=0$).

TABLE 1 THERMO PHYSICAL PROPERTIES OF WATER AND THE ELEMENTS CU, AG AND AL2O3 [13]

properties	fluid (water)	Cu	Ag	Al ₂ O ₃
C_p (j/kgK)	4179	385	235	765
ρ (kg/m ³)	997.1	8933	10500	3970
K (W/mK)	0.613	400	429	40
$\alpha \times 10^7$ (m ² /s)	1.47	1163.1	1738.6	131.7

Similarity Transformation

In this section, we introduce the following dimensionless functions f, g and θ and the similarity variable η

$$\left. \begin{aligned} \eta = \sqrt{\frac{a}{\nu_f(1-\gamma)}} z, \quad u = \left(\frac{ax}{1-\gamma} \right) f'(\eta), \quad v = \left(\frac{ay}{1-\gamma} \right) g'(\eta), \\ w = -\sqrt{a\nu}(f + g) \quad \theta(\eta) = \frac{T - T_\infty}{T_w - T_\infty} \end{aligned} \right\} \quad (7)$$

where ν_f is the kinematic viscosity of the base (water), substituting (7) into eqs. (2-4), we obtain

$$\left[\frac{1}{(1-\phi)^{2.5} \left(1 - \phi + \phi \frac{\rho_s}{\rho_f} \right)} \right] f''' + (f+g)f'' - f'^2 - A \left(f' + \frac{\eta}{2} f'' \right) = 0 \quad (8)$$

$$\left[\frac{1}{(1-\phi)^{2.5} \left(1 - \phi + \phi \frac{\rho_s}{\rho_f} \right)} \right] g''' + (f+g)g'' - g'^2 - A \left(g' + \frac{\eta}{2} g'' \right) = 0 \quad (9)$$

$$\left[\frac{\left(\frac{k_{nf}}{k_f} \right)}{p_r \left(1 - \phi + \phi \frac{(\rho C_p)_s}{(\rho C_p)_f} \right)} \right] \theta'' + (f+g)\theta' - (f'+g')\theta - A \left(\theta + \frac{\eta}{2} \theta' \right) = 0 \quad (10)$$

where $A = \left(\frac{\gamma}{a} \right)$ is the unsteadiness parameter, $p_r = \left(\frac{\nu \rho C_p}{k} \right)_f$ is the prandtl number.

The boundary condition (5) become

$$\left. \begin{aligned} f(0) + g(0) &= fw, \quad f'(0) = 1, \quad g'(0) = \zeta, \quad \theta(0) = 1 \\ f'(\infty) &= 0, \quad g'(\infty) = 0, \quad f''(\infty) = 0, \quad g''(\infty) = 0, \quad \theta(\infty) = 0 \end{aligned} \right\} \quad (11)$$

where fw is the suction/injection parameter and $(\zeta = b/a)$ is the stretching ratio parameter, and when $(\zeta = 0)$ the problem reduces to the two-dimensional case $[g = 0]$, and when $(\zeta = 1)$ the problem reduces to the axisymmetric flow $[f=g]$

Numerical Solutions and Results

We first convert the Equations (8),(9) and (10) to a system of differential equations of first order , by using

$$\begin{aligned} S_1 &= f, \quad S_2 = f', \quad S_3 = f'', \quad S_4 = g, \quad S_5 = g', \quad S_6 = g'', \quad S_7 = \theta, \quad S_8 = \theta' \\ \left. \begin{aligned} S_1' &= S_2 \\ S_2' &= S_3 \\ S_3' &= B \left[S_2^2 - (S_1 + S_4)S_3 + A \left(S_2 + \frac{\eta}{2} S_3 \right) \right] \\ S_4' &= S_5 \\ S_5' &= S_6 \\ S_6' &= B \left[S_5^2 - (S_1 + S_4)S_6 + A \left(S_5 + \frac{\eta}{2} S_6 \right) \right] \\ S_7' &= S_8 \\ S_8' &= \left(\frac{P_r}{D} \right) \left[(S_2 + S_5)S_7 - (S_1 + S_4)S_8 + A \left(S_7 + \frac{\eta}{2} S_8 \right) \right] \end{aligned} \right\} \quad (12) \end{aligned}$$

Where $B = (1 - \phi)^{2.5} \left(1 - \phi + \phi \frac{\rho_s}{\rho_f} \right)$ and $D = \frac{\left(\frac{k_{nf}}{k_f} \right)}{\left(1 - \phi + \phi \frac{(\rho C_p)_s}{(\rho C_p)_f} \right)}$

Subjected to the initial conditions

$$\left. \begin{aligned} S_1(0) + S_4(0) = fw, \quad S_2(0) = 1, \quad S_3(0) = m, \quad S_5(0) = \zeta, \quad S_6(0) = n \\ S_7(0) = 1, \quad S_8(0) = \ell \end{aligned} \right\} \quad (13)$$

where m , n and ℓ are unknown to be determined as a part of the numerical solution.

Using Mathematica program, a function (F) has been defined such that $F [m_ , n_ , \ell_] := \text{NDSolve} [\text{system (12),(13)}]$, The value of m , n and ℓ are determined upon solving the equations, $S_2(\eta_{\max}) = 0$, $S_5(\eta_{\max}) = 0$ and $S_7(\eta_{\max}) = 0$ to get the solution, NDSolve first searches for initial conditions that satisfy the equations, using a combination of Solve and a procedure much like Find Root. Once m , n and ℓ are determined the system (12) and (13) is closed, it can be solved numerically using the NDSolve function based on Runge-Kutta technique.

From the engineering point of view, the most important characteristics of the flow are the skin friction coefficient, and Nusselt number which are indicate physically to surface shear stress, and rate of heat transfer respectively. These characteristics effect directly on the mechanical properties of the surface during the heat treatment process, such that increasing the rate of heat transfer from the surface accelerates the cooling of the surface which improve the hardness and shear strength of the surface but on the other hand decrease the ductility of the surface and increase surface cracking.

3.1 Surface Shear Stress

Surface shear stress along the x-axis is

$$\tau_w(x) = \mu_{nf} \left(\frac{\partial u}{\partial z} \right)_{z=0} = \frac{\mu_f U_w}{(1 - \phi)^{2.5}} \sqrt{\frac{a}{\nu_f (1 - \phi)}} f''(0) \quad (14)$$

Surface shear stress along the y-axis is

$$\tau_w(y) = \mu_{nf} \left(\frac{\partial v}{\partial z} \right)_{z=0} = \frac{\mu_f V_w}{(1 - \phi)^{2.5}} \sqrt{\frac{a}{\nu_f (1 - \phi)}} g''(0) \quad (15)$$

Since the skin friction coefficient is given by

$$C_f = \frac{2\tau_w}{\rho U_w^2} \quad \text{i.e.} \quad f''(0) = \frac{1}{2} C_f \sqrt{R_e} (1 - \phi)^{2.5} \quad g''(0) = \frac{1}{2} \left(\frac{U_w}{V_w} \right) C_f \sqrt{R_e} (1 - \phi)^{2.5} \quad (16)$$

3.2 Surface Heat Flux

$$q_w = -k_{nf} \left(\frac{\partial T}{\partial y} \right)_{z=0} = -k_{nf} (T_w - T_\infty) \sqrt{\frac{a}{\nu_f (1 - \phi)}} \theta'(0) \quad (17)$$

Since the Nusselt number is given by

$$Nu = \frac{xq_w}{k_f (T_w - T_\infty)} \quad \text{i.e.} \quad Nu = - \left(\frac{k_{nf}}{k_f} \right) \sqrt{R_e} \theta'(0) \quad (18)$$

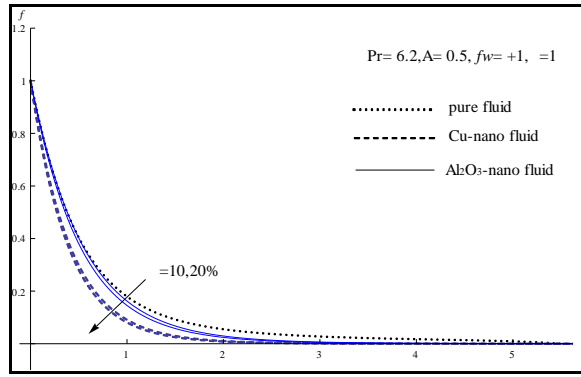


FIGURE 2 THE VELOCITY PROFILE WITH INCREASING OF NANOPARTICLE VOLUME FRACTION (ϕ).

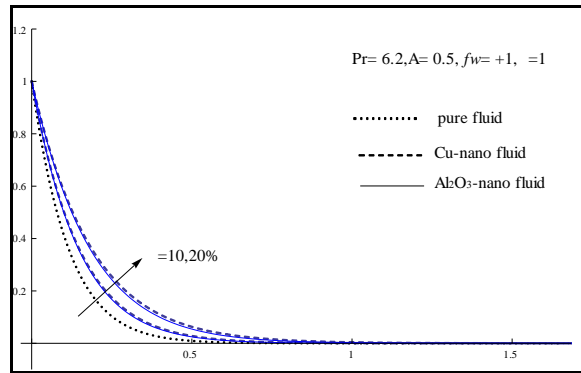


FIGURE 3 THE TEMPERATURE PROFILE WITH INCREASING OF NANOPARTICLE VOLUME FRACTION (ϕ)

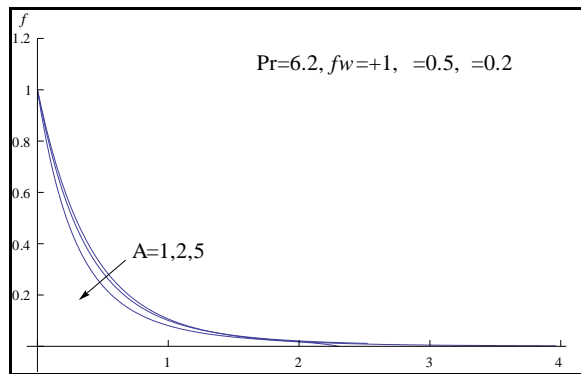


FIGURE 4 THE VELOCITY PROFILE WITH INCREASING OF UNSTEADINESS PARAMETER (A)

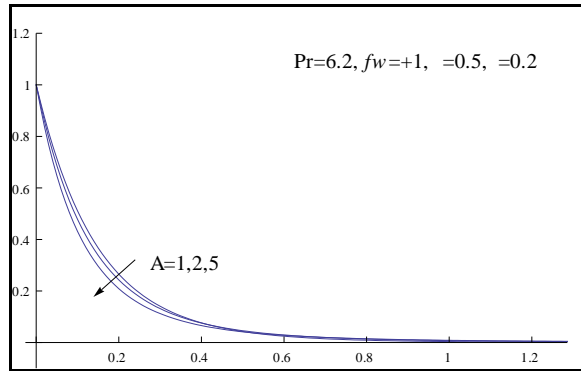


FIGURE 5 THE TEMPERATURE PROFILE WITH INCREASING OF UNSTEADINESS PARAMETER (A)

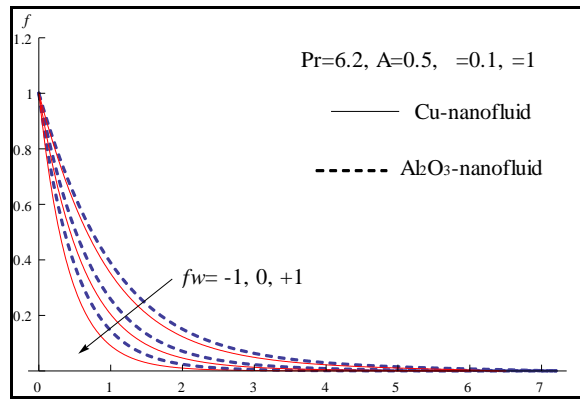


FIGURE 6 THE VELOCITY PROFILE WITH INCREASING OF SUCTION/INJECTION PARAMETER (fw).

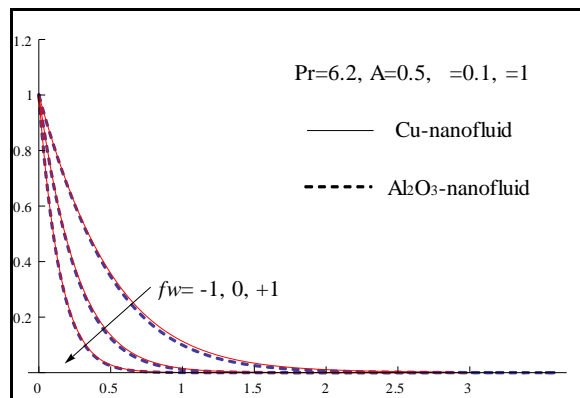


FIGURE 7 THE TEMPERATURE PROFILE WITH INCREASING OF SUCTION/INJECTION PARAMETER (fw).

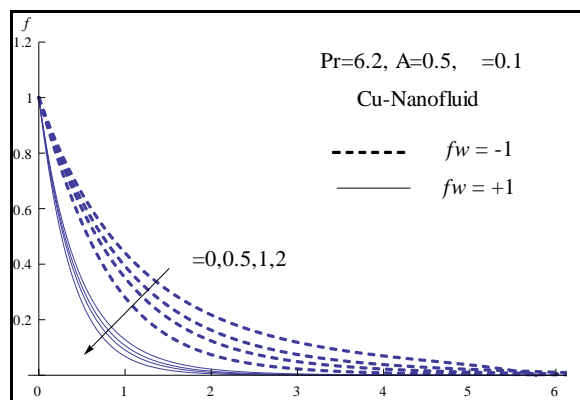


FIGURE 8 THE VELOCITY PROFILE WITH INCREASING OF STRETCHING PARAMETER (λ).

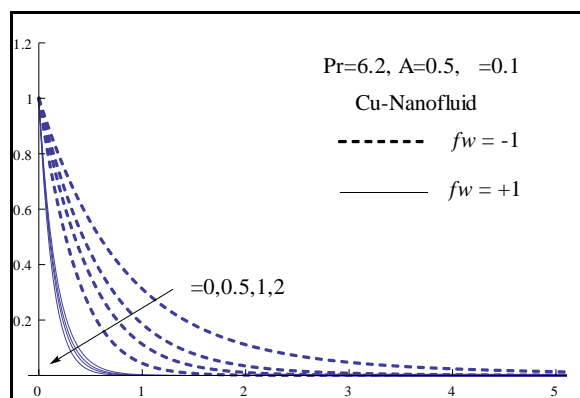


FIGURE 9 THE TEMPERATURE PROFILE WITH INCREASING OF STRETCHING PARAMETER (λ).

TABLE 2 COMPRESSIONS THE VALUES OF VELOCITY GRADIENT WITH PREVIOUS PUBLICATION

ζ	Gireesha et al. [19]		Present results	
	$-f''(0)$	$-g''(0)$	$-f''(0)$	$-g''(0)$
0	-1.0000	0.0000	-1.0000	0.0000
0.5	-1.22474	-0.61237	-1.22474	-0.61237
1.0	-1.41421	-1.41421	-1.41420	-1.41420

TABLE 3 VALUES OF VELOCITY GRADIENT AND TEMPERATURE GRADIENT AT THE SURFACE AT $z=0.5$, $Pr = 6.2$ FOR (Cu-WATER)

A	fw	φ	(Cu-Water) Nano fluid					
			$-f''(0)$	$-g''(0)$	$-\theta'(0)$	Cfx	Cfy	Nu
0	-1	0	0.68017	0.24907	1.35067	0.00192	0.00018	955.07
		0.1	0.73789	0.26216	1.28640	0.00272	0.00024	1211.29
		0.2	0.75406	0.26341	1.21778	0.00373	0.00033	1503.23
	1	0	1.71424	0.79468	8.02731	0.00485	0.00056	5676.16
		0.1	2.23641	1.10773	6.14887	0.00823	0.00102	5789.67
		0.2	2.28139	1.06947	4.83867	0.01127	0.00132	5972.86
1	-1	0	0.98678	0.42628	1.93700	0.00279	0.00030	1369.67
		0.1	1.09433	0.46829	1.80291	0.00403	0.00043	1697.59
		0.2	1.11902	0.47787	1.67331	0.00553	0.00059	2065.54
	1	0	1.94907	0.91985	8.34921	0.00551	0.00065	5903.79
		0.1	2.42671	1.15154	6.47560	0.00893	0.00106	6097.32
		0.2	2.55155	1.21233	5.12834	0.01261	0.00150	6330.43
2	-1	0	1.24314	0.56660	2.45644	0.00352	0.00040	1736.96
		0.1	1.39213	0.63135	2.26217	0.00512	0.00058	2130.03
		0.2	1.42701	0.64650	2.07939	0.00705	0.00080	2566.80
	1	0	2.17188	1.03785	8.67181	0.00614	0.00073	6131.90
		0.1	2.67953	1.28483	6.78160	0.00986	0.00118	6385.45
		0.2	2.81132	1.34912	5.41840	0.01389	0.00167	6688.48

TABLE 4 VALUES OF VELOCITY GRADIENT AND TEMPERATURE GRADIENT AT THE SURFACE AT $z=0.5$, $Pr = 6.2$ FOR (Ag-WATER)

A	fw	φ	(Ag-Water) Nano fluid					
			$-f''(0)$	$-g''(0)$	$-\theta'(0)$	Cfx	Cfy	Nu
0	-1	0	0.68017	0.24907	1.35067	0.00192	0.00018	955.07
		0.1	0.75223	0.26496	1.27865	0.00277	0.00024	1204.10
		0.2	0.76954	0.26803	1.20172	0.00380	0.00033	1483.65
	1	0	1.71424	0.79468	8.02731	0.00485	0.00056	5676.16
		0.1	2.37886	1.17988	6.00561	0.00876	0.00109	5655.42
		0.2	2.48551	1.16895	4.61249	0.01228	0.00144	5694.58
1	-1	0	0.98678	0.42628	1.93700	0.00279	0.00030	1369.67
		0.1	1.12294	0.47939	1.78954	0.00413	0.00044	1685.19
		0.2	1.15851	0.49308	1.64594	0.00572	0.00061	2032.08
	1	0	1.94907	0.91985	8.34921	0.00551	0.00065	5903.79
		0.1	2.57199	1.22228	6.33455	0.00947	0.00112	5965.18
		0.2	2.76616	1.31699	4.90363	0.01367	0.00163	6054.03
2	-1	0	1.24314	0.56660	2.45644	0.00352	0.00040	1736.96
		0.1	1.43258	0.64892	2.24418	0.00527	0.00060	2113.32
		0.2	1.48322	0.67082	2.04330	0.00733	0.00083	2522.67
	1	0	2.17188	1.03785	8.67181	0.00614	0.00073	6131.90
		0.1	2.83288	1.35964	6.64092	0.01043	0.00125	6253.69
		0.2	3.03711	1.45941	5.19470	0.01501	0.00180	6413.38

TABLE 5 VALUES OF VELOCITY GRADIENT AND TEMPERATURE GRADIENT AT THE SURFACE AT z=0.5, PR = 6.2 FOR (AL₂O₃-WATER)

A	fw	φ	(Al ₂ O ₃ -Water) nano fluid					
			- f''(0)	- g''(0)	- θ'(0)	Cfx	Cfy	Nu
0	-1	0	0.68017	0.24907	1.35067	0.00192	0.00018	955.07
		0.1	0.68091	0.25231	1.29690	0.00251	0.00023	1207.65
		0.2	0.66354	0.24482	1.23810	0.00328	0.00030	1495.86
	1	0	1.71424	0.79468	8.02731	0.00485	0.00056	5676.16
		0.1	1.71060	0.79293	6.24042	0.00630	0.00073	5810.98
		0.2	1.66309	0.81896	4.92428	0.00822	0.00101	5949.47
1	-1	0	0.98678	0.42628	1.93700	0.00279	0.00030	1369.67
		0.1	0.98475	0.42511	1.81555	0.00362	0.00039	1690.61
		0.2	0.95556	0.41326	1.69314	0.00472	0.00051	2045.64
	1	0	1.94907	0.91985	8.34921	0.00551	0.00065	5903.79
		0.1	1.94517	0.91796	6.54003	0.00716	0.00084	6089.97
		0.2	1.83566	0.86506	5.22030	0.00907	0.00107	6307.13
2	-1	0	1.24314	0.56660	2.45644	0.00352	0.00040	1736.96
		0.1	1.23993	0.56481	2.27507	0.00456	0.00052	2118.51
		0.2	1.20038	0.54733	2.09879	0.00593	0.00068	2535.74
	1	0	2.17188	1.03785	8.67181	0.00614	0.00073	6131.90
		0.1	2.16761	1.03577	6.84044	0.00798	0.00095	6369.72
		0.2	2.05027	0.97885	5.49895	0.01013	0.00121	6643.79

TABLE 6 VALUES OF VELOCITY GRADIENT AND TEMPERATURE GRADIENT AT THE SURFACE AT z=1, PR = 6.2 FOR (CU-WATER)

A	fw	φ	(Cu-Water) Nano fluid					
			- f''(0)	- g''(0)	- θ'(0)	Cfx	Cfy	Nu
0	-1	0	0.73826	0.73826	1.75221	0.00209	0.00104	1239.00
		0.1	0.80043	0.80043	1.64954	0.00295	0.00147	1553.23
		0.2	0.81367	0.81367	1.54562	0.00402	0.00201	1907.92
	1	0	1.79867	1.79867	8.48219	0.00509	0.00254	5997.82
		0.1	2.35489	2.35489	6.54104	0.00867	0.00433	6159.10
		0.2	2.38242	2.38242	5.17783	0.01177	0.00589	6391.53
1	-1	0	1.02831	1.02831	2.27957	0.00291	0.00145	1611.90
		0.1	1.13951	1.13951	2.10851	0.00419	0.00210	1985.39
		0.2	1.16475	1.16475	1.94610	0.00576	0.00035	2402.27
	1	0	2.01672	2.01672	8.77947	0.00570	0.00285	6208.02
		0.1	2.50680	2.50680	6.84070	0.00923	0.00461	6441.27
		0.2	2.63438	2.63438	5.44155	0.01302	0.00271	6717.06

TABLE 7 VALUES OF VELOCITY GRADIENT AND TEMPERATURE GRADIENT AT THE SURFACE AT Z=1, Pr = 6.2 FOR (AG-WATER)

A	fw	ϕ	(Ag-Water) Nano fluid					
			$-f''(0)$	$-g''(0)$	$-\theta'(0)$	C_{fx}	C_{fy}	Nu
0	-1	0	0.73826	0.73826	1.75221	0.00209	0.00104	1239.00
		0.1	0.81574	0.81574	1.63750	0.00300	0.00150	1542.02
		0.2	0.83410	0.83410	1.52014	0.00412	0.00206	1876.78
	1	0	1.79867	1.79867	8.48219	0.00509	0.00254	5997.82
		0.1	2.40234	2.40234	6.41240	0.00884	0.00442	6038.50
		0.2	2.59172	2.59172	4.93907	0.01281	0.00640	6097.81
1	-1	0	1.02831	1.02831	2.27957	0.00291	0.00145	1611.90
		0.1	1.12753	1.12753	1.98965	0.00415	0.00208	1873.64
		0.2	1.20966	1.20966	1.91004	0.00598	0.00299	2358.14
	1	0	2.01701	2.01701	8.77942	0.00570	0.00285	6207.99
		0.1	2.65531	2.65531	6.69241	0.00977	0.00489	6302.18
		0.2	2.85389	2.85389	5.20399	0.01410	0.00705	6424.88

TABLE 8 VALUES OF VELOCITY GRADIENT AND TEMPERATURE GRADIENT AT THE SURFACE AT Z=1, Pr = 6.2 FOR (AL2O3-WATER)

A	fw	φ	(Al ₂ O ₃ -Water) Nano fluid					
			$-f''(0)$	$-g''(0)$	$-\theta'(0)$	C_{fx}	C_{fy}	Nu
0	-1	0	0.73826	0.73826	1.75221	0.00209	0.00104	1239.00
		0.1	0.73766	0.73766	1.66673	0.00272	0.00136	1552.03
		0.2	0.72022	0.72022	1.57376	0.00356	0.00178	1901.41
	1	0	1.79867	1.79867	8.48219	0.00509	0.00254	5997.82
		0.1	1.79491	1.79491	6.64115	0.00661	0.00330	6184.13
		0.2	1.68956	1.68956	5.29667	0.00835	0.00417	6399.40
1	-1	0	1.02831	1.02831	2.27957	0.00291	0.00145	1611.90
		0.1	1.02570	1.02570	2.12631	0.00378	0.00189	1979.99
		0.2	0.99563	0.99563	1.97366	0.00492	0.00246	2384.56
	1	0	2.01667	2.01667	8.77948	0.00570	0.00285	6208.03
		0.1	2.01266	2.01266	6.91566	0.00741	0.00370	6439.75
		0.2	1.90011	1.90011	5.54940	0.00939	0.00469	6704.75

Discussion

We present in this study , three dimensional mathematical model of a moving continuous surface embedded into a Nanofluid. The influence of nanoparticle type, Nanoparticles volume fraction (ϕ), suction/injection parameter (fw), stretching parameter (ζ), and the unsteadiness parameter (A) on the velocity and the temperature within the boundary layer are shown in figures (2-9). Moreover, we considered three different types of nanoparticles, Cu, Ag and Al₂O₃ with water as the base fluid. Table (1) shows the thermo physical properties of water and the elements Cu, Ag and Al₂O₃. The prandlt number of the base fluid (water) kept constant at 6.2.

The effect of Nanoparticles concentration (volume fraction) (ϕ) on the velocity and temperature of the boundary layer of (Cu and Al₂O₃) Nanofluid are shown in figures (2) and (3) respectively. It observed that the increases of nanoparticle volume fraction decrease the velocity but increase the temperature of the boundary layer. Also one can observe that the velocity for (Al₂O₃- water) is higher than that for (Cu-water).

The effect of unsteadiness parameter (A) on the velocity and temperature of the boundary layer of (Cu-Nanofluid) showed in figures (4) and (5) respectively. It observed that the increases of unsteadiness parameter decrease both the velocity and the temperature of the boundary layer.

Figures (6) and (7) show the effect of suction/injection parameter on the velocity and temperature of (Cu and Al₂O₃) Nanofluid boundary layer, respectively. It observed that the increases of suction/injection parameter decrease both the velocity and the temperature of the boundary layer. In addition, one can observe that the velocity for (Al₂O₃-water) is higher than that for (Cu-water) in the case of suction and injection

The effect of stretching parameter (ζ) on the velocity and temperature of the boundary layer of (Cu-Nanofluid) showed in figures (8) and (9) respectively. It observed that the increases of stretching parameter decrease both the velocity and temperature of the boundary layer. In addition, it is clear that the injection process has high velocity and temperature compared with suction. Also one can say that the velocity and temperature in 2-D problem ($\zeta=0$) are high compared to the 3-D problem ($\zeta\neq 0$).

Tables (2-4) shows the values of velocity gradient and temperature gradient at the surface and the corresponding values of skin friction and Nusselt number for different values of (A), (fw) and (ϕ) at $Re = 5 \times 10^5$. The effect of Nanoparticles type, concentration of Nanoparticles within the base fluid, steady and unsteady motion, suction /injection and the stretching velocity in each direction on surface shear stress, surface heat flux and mechanical properties (hardness, stiffness, strength, surface cracking, etc.) discussed below.

Type of Nano-particles

It is clear from tables (3-5) that the values of velocity gradient at the surface increased gradually by changing the nanoparticle from Al₂O₃ to Cu to Ag. Nevertheless, the opposite effect occurs on temperature gradient. On the other hand, the skin friction and surface shear stress are higher in the case of Ag-Nanofluid than that in Cu and Al₂O₃-nanofluid, also the Nusselt number and rate of heat transfer from the surface are higher in the case of Cu-Nanofluid than that in Al₂O₃ and Ag-Nanofluid, which means that using Cu-Nanofluid as a cooling medium is more useful for the surface hardness and strength.

In general using a Nanofluid in the cooling process is more active to improve the mechanical properties of the surface, such that using Nanofluid increase the rate of heat transfer by (12-38%) more than in the case of pure water that leads to accelerate the cooling of the surface which increase the surface hardness and strength

Concentration of Nano-particle Within the Base Fluid

Tables (3-5) shows that the values of velocity gradient at the surface increase gradually by increasing the particle volume fraction from 10% to 20% in the case of Cu and Ag-nanoparticle and decrease for Al₂O₃ nanoparticle, but the temperature gradient decreases by increase of it for all types of nanoparticles.

On the other hand the skin friction and Nusselt number both increase with increasing of the concentration of nanoparticle within the base fluid. Therefore, one can say that the Nanofluid with 20% nanoparticle is more effective on the mechanical properties than that with 10% nanoparticle.

Steady and Unsteady Motion

It is clear that the unsteady motion of the surface has a direct effect on the mechanical properties such that increase the unsteadiness parameter increase the velocity gradient, skin friction, and surface shear stress also increase the temperature gradient, Nusselt number, and rate of heat transfer. It is worth mentioning that increasing the unsteadiness parameter from 0 to 2 increases the rate of heat transfer from the surface by 12% for all types of nanoparticles.

Suction and Injection Process

One can say that the suction/injection process has an important effect in the cooling process, such that in the case of suction the velocity gradient, skin friction, surface shear stress, temperature gradient, Nusselt number and rate of heat transfer all are higher than that in the case of injection. As we know from previous the increase the rate of heat transfer from the surface improve the mechanical properties of surface.

Stretching Velocity in Each Direction

By comparing the values of tables (3-5) at $\zeta=0.5$ and tables (6-8) at $\zeta=1$, we observed that increasing the stretching velocity in y -direction relative to x -direction increase the values of velocity gradient, skin friction, surface shear stress, temperature gradient, Nusselt number and rate of heat transfer parameter which leads to improving the mechanical properties of the surface

Conclusions

We present in this study a three dimensional mathematical model of a continuous moving surface embedded into a Nanofluid, the study based on three types of nanoparticle that are the most used types (Cu, Ag, and Al₂O₃). The mechanical properties of the surface were our goal in this study and the following results obtained:

- Using Nanofluid as a cooling medium is useful to improve the mechanical properties by (12-38%) according to the type of nanoparticles used.
- Here we studied three types only of Nanoparticles, according to this study the best type used to improve the mechanical properties of the surface is Cu-Nanofluid and the best type used to decrease the surface shear stress is Al₂O₃-nanofluid, and from the side of the cost Al₂O₃ is the best type used.
- Using nanoparticle in a base fluid with concentration of 20% is more effect than that of 10%.
- Transform the motion from steady to unsteady leads to increasing the values of velocity and temperature gradient, which leads to increase of skin friction and rate of heat transfer.
- Cooling with suction is more effect on skin friction and rate of heat transfer than that with injection.
- Stretching the surface in two directions is more effect on skin friction and rate of heat transfer than that stretching in one direction.

REFERENCES

- [1] Choi, S.U.S., "Enhancing thermal conductivity of fluids with Nanoparticles," The proceedings of the 1995 ASME International Mechanical Engineering Congress and Exposition, San Francisco, USA. ASME, FED 231/MD 66, (1995) pp. 99-105.
- [2] Yacob, N.A., Ishak, A., Nazar, R. and Pop, I., "Boundary layer flow past a stretching/ shrinking surface beneath an external uniform shear flow with a convective surface boundary condition in a Nanofluid," *Nanoscale Research Letters*, 6, (2011) pp. 1-7.
- [3] Aminreza, N., Rashid, P., and Mohamed, G., "Effect of partial slip boundary condition on the flow and heat transfer of Nanofluid past stretching sheet prescribed constant wall temperature," *International Journal of thermal Science*, (2012) pp. 1-9.
- [4] Rana, P. and Bhargava, R., "Flow and heat transfer of a Nanofluid over a nonlinearly stretching sheet," *Communication Nonlinear Science Numer*, 17, (2012), pp 212-226.
- [5] Alsaedi, A., Awais, M. and Hayat, T., "Effects of heat generation/absorption on stagnation point flow of Nanofluid over a surface with convective boundary conditions," *Communication Nonlinear Science Numer*, 17, (2012) ,pp. 4210-4223.
- [6] Hamad, M., "Analytical solution of natural convection flow of Nanofluid over a linearly stretching sheet in the presence of magnetic field," *International communications in heat and mass transfer*, 38, (2011), pp. 487-492.
- [7] Aziz, A. and Khan, W.A., "Natural convective boundary layer flow of a Nanofluid past a convectively heated vertical plate," *International Journal of Thermal Sciences*, 52, (2012), pp. 83-90.
- [8] Fang, T., Zhang, J. and Yong fang, Z., "Boundary layer flow over a stretching sheet with variable thickness," *Applied Mathematics and Computation*, 218, (2012), pp. 7241-7252.

- [9] Elbashbeshy, E.M.A., Emam, T. G. and Abdelwahed, M. S., "An exact solution of boundary layer flow over a moving surface embedded into a Nanofluid in the presence of magnetic field and suction/injection," *Heat Mass Transfer*, 50(1), (2014), pp. 57-64.
- [10] Elbashbeshy, E.M.A., Emam, T. G. and Abdelwahed, M. S., "Effect of magnetic field on flow and heat transfer of a Nanofluid over an unsteady continuous moving surface in the presence of suction/injection," *International Journal of Applied Mathematics*, 14(10), (2012), pp. 436-442.
- [11] Elbashbeshy, E.M.A., Emam, T. G. and Abdelwahed, M. S., "Flow and heat transfer over a moving surface with non-linear velocity and variable thickness in a Nanofluid in the presence of thermal radiation," *Canadian journal of Physics* 92(2), (2014), pp. 124-130.
- [12] Elbashbeshy, E.M.A., Emam, T. G. and Abdelwahed, M. S., "The effect of thermal radiation and heat generation on the mechanical properties of unsteady continuous moving cylinder in a Nanofluid in the presence of suction or injection," *Thermal science*, 19(5), (2015), pp. 1591-1601.
- [13] Elbashbeshy, E.M.A., Emam, T. G. and Abdelwahed, M. S., "Effect of heat treatment process with a new cooling medium (Nanofluid) on the mechanical properties of an unsteady continuous moving cylinder," *Journal of Mechanical science and technology*, 27(12), (2013), pp. 3843-3850.
- [14] Nazar, R. and Latip, A., "Numerical investigation of three dimensional boundary layer flows due to a stretching surface in a viscoelastic fluid," *European Journal of Scientific Research*, 29(4), (2009), pp. 509-517.
- [15] Takhar, H. and Nath, S.G., "Unsteady three dimensional MHD boundary layer flow due to the impulsive motion of a stretching surface," *Acta Mechanica*, 146, (2001), pp. 59-71.
- [16] Nabil, T. E., Elsaka, A.G., Radwan, A. E., and Magdy, A. E., "Three dimensional flow over a stretching surface in a viscoelastic fluid with heat and mass transfer," *Nature and Science Journal* 8(8), (2010), pp. 218-228.
- [17] Aboeldahab, E.M. and Azzam, G.E.D.A., "Unsteady three dimensional MHD combined heat and mass free convective flow over a stretching surface with time dependent chemical reaction," *Acta Mechanica*, 184, (2006), pp.121-136.
- [18] Elbashbeshy, E.M.A., Emam, T. G. and Abdelwahed, M. S., "Three dimensional flow over a stretching surface with thermal radiation and heat generation in the presence of chemical reaction and suction/injection," *International Journal of Energy & Technology* 3 (16), (2011), pp. 1-8.
- [19] Gireesha B. J. , Mahanthesh B., Rama S. R. G., and Manjunatha P. T., "Thermal radiation and Hall effects on boundary layer flow past a non-isothermal stretching surface embedded in porous medium with non-uniform heat source/sink and fluid-particle suspension," *Heat Mass Transfer*, 4(52), (2016), pp. 897-911
- [20] Mahanthesh B., Gireesha B.J., Rama S. R. G., "Nonlinear radiative heat transfer in MHD three-dimensional flow of water based nanofluid over a non-linearly stretching sheet with convective boundary condition," *Journal of the Nigerian Mathematical Society* 35, (2016), pp. 178-198
- [21] Mahanthesh B., Gireesha B.J., Gorla R.S. R., Abbasi F.M., and Shehzad S.A., "Numerical solutions for magnetohydrodynamic flow of nanofluid over a bidirectional non-linear stretching surface with prescribed surface heat flux boundary," *Journal of Magnetism and Magnetic Materials* 417, (2016), pp. 189-196

DVD Algorithm Based On Nearest Neighbor For WSN

Dr. D. USHA*¹

Mother Teresa Women's University, Kodaikanal, Tamilnadu India

*ushadanabal@gmail.com

Abstract

Wireless Sensor Networks has augmented technological growth. Wireless networks collect critical data and transmit them to assist in taking decisions. The applications of WSNs can be in patient health monitoring system and fire detection system. Transmitted data needs to be accurate as they are deployed in mission-critical applications. , WSN communications can be affected by Hostile environments like forest fires and they are vulnerable to abnormalities. These differential values affect quality of collected data and need to be addressed. This paper suggests a new distance based Differential Value Detection Algorithm (DVD) for WSNs to identify abnormalities in WSN node readings.

Keywords

Differential Value Detection Algorithm; WSN; Intrusion Detection; Nearest Neighbor

1. Introduction

Wireless Sensor Networks (WSNs) is a collection of sensor nodes managed by sinks. The Sensor nodes communicate using intermediate nodes, which collect and transmit information from their surroundings to the sink. These WSN networks are employed in many situations like military surveillance, building automations etc. This transmitted data is of high importance [1]. Though WSN nodes energy resource is very less [2]. They can be deployed when there is difficulty in deploying wired networks. Anomalies are interpretations that do not correspond to defined behaviors [3]. Several studies have been conducted on Anomaly Detection Techniques in WSNs like Distributed Sensor Networks [4], SVMs [5], online sensor techniques [6], WSN maps and wavelets [7], Outlier Event Detection [8]. This paper proposes a detection algorithm DVD, to detect abnormalities in node signals using the nearest neighbor NN technique. The data is processed in a single pass, differentiating it from other algorithms. The DVD algorithm can maintain accuracy even in data varying with time and the updates are simple and fast, since DVD.

2. Research Objective

Signals generated from WSN nodes is infinite and off-line learning algorithms may not help in finding deviations, during results analysis. Moreover, most node signal values are constant and abnormalities in their values are rare Node information is evolved over a period time and needs to be checked for differential values. The objective of this paper is to check differences in node readings and report them to the sink.

3. Differential Values in Data or Outliers

Grubbs stated that any value deviating from other values in a sample, is an anomaly. If they are not investigated, important data may be lost, thus implying the need to identify and study these anomalies Erroneous data, due to abnormalities can result in incorrect assumptions, specifically in statistical analysis or data mining investigations. These abnormalities or outliers can be deleted without investigation, which again is a risk. There are numerous tests like Rosner, Grubbs, box plot rule and Dixon test, for identifying such abnormalities. They are non-regression methods based on hypothetical testing and classes [9]. Abnormal data can be detected using distance-based approaches. Though, distribution-based statistical models [10] can be applied to select data instances for identifying outliers, multidimensional datasets cannot be used to recognize outliers using distribution-based

approaches. Figure 1 depicts Outliers.

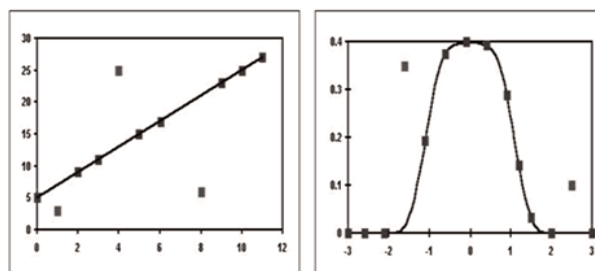


FIGURE 1. OUTLIERS

4. Outlier Detection

There is no proper definition of an outlier, as it is an observation in a pool of data and subjective to the data in which it exists. Outliers are found [11] without prior knowledge of the data. Outliers can also be found on irregular, but normalized data. One approach of equalizing data from outliers is by eliminating them. Outlier approaches assume that the data is normalized and evenly distributed, apply mean and standard deviations on this data, before identifying data values that are abnormal. Density-based outlier approaches [12] compute and identify dense and sparse regions in data and stress that sparse regions are outliers. The distance of the data points from a Local Outlier Factor (LOF) is considered while identifying outliers [13]. R. Fagin et.al., identified outliers based on computational geometry in [14]. The model failed on high dimensional data sets.

5. Differential Value Detection Algorithm

The nearest-neighbor method is assumed to be slow in higher dimensional data sets, since, in high-dimensional spaces, points tend to be far away from each other and NN classifier may be less meaningful. The Differential Value Detection Algorithm is a technique that considers the average in a set of values, to minimize the number of iterations. It uses NN classifier to classify abnormalities even in high-dimensional datasets. DVD is experimented with node signal values (Transactions), to detect outliers. WSNs perform millions of transactions with thousands of nodes. The objective of DVD is to identify anomalous transactions in node value patterns of WSN data, using nearest neighbor algorithm. An indoor node transmitting humidity and temperature when viewed as a transaction may have the following parameters (1) Reading#, (2) Mote-ID (3) Humidity, (4) Temperature and optionally a Label as the fifth parameter. The Training samples are built using node signal values of WSN nodes. Each Transaction or reading (Node parameter value) is an instance. The NN Algorithm to identify outliers in Node Signal Values is listed below.

5.1 NN Algorithm to Identify Outliers in Node Signal Values

// Distance between samples in N

Let the Node Signal Value be called the NSigVal.

Let the MaxNSigVal in the Range be defined as $NSigVal + 5\%$ of NSigVal

Let the MinNSigVal in the Range be defined as $NSigVal - 5\%$ of NSigVal

$NTestSigVal = NSigVal$ //The First Value is taken as E

For $i = 1$ to M //M is the Number of Transactions of Node Signals

within a Specified Time Period

$NMaxSigVal = NTestSigVal + 5\%$ of $NTestSigVal$

$NMinSigVal = NTestSigVal - 5\%$ of $NTestSigVal$

For $j=i+1$ n to M

If (NSigVal > NTestSigVal and NSigVal <=NMaxSigVal)

“Store”

End if //

If (NSigVal < NTestSigVal and NSigVal >=NMaxSigVal)

“Store”

End if //.

If (NSigVal > NMaxSigVal or NSigVal < NMinSigVal)

“Store Differential Reading”

End if

End of J

NTestSig = NSigVal //Each Signal Value is taken as the next E

End of I

The transactions of for one Node with id 1 is listed in Table 1.

TABLE 1. MOTEID 1 READINGS

Reading#	Mote ID	Humidity	Temperature
1	1	44.45	27.81
2	1	44.42	27.81
3	1	44.42	27.81
4	1	44.38	27.8
5	1	44.35	27.79
6	1	44.32	27.77
7	1	44.38	27.74
8	1	44.52	27.73
9	1	44.65	27.72
10	1	44.71	27.73
11	1	44.85	27.73
12	1	44.78	27.74
13	1	44.71	27.73
14	1	45.18	27.75
15	1	46.26	27.84
16	1	49.26	27.98
17	1	53.06	28.11
18	1	51.12	28.27
19	1	49.48	28.4
20	1	74.17	36.39
21	1	82.61	41.45
22	1	82.79	45.53
23	1	75.74	49.9
24	1	66.97	54.08
25	1	44.45	27.81
26	1	44.42	27.81
27	1	44.42	27.81
28	1	44.38	27.8
29	1	44.35	27.79
30	1	44.32	27.77
31	1	44.38	27.74
32	1	44.52	27.73

The NN iterations for classifying Outliers would be the sum of 32 + 31 + 30 + 29 + 28 + 27 + 26 +1. Each instance computes an (LOF) creating considerations for an outlier. Taking the First humidity value 44.45 as an example, the distances of transactions from the median is depicted in Figure 2.

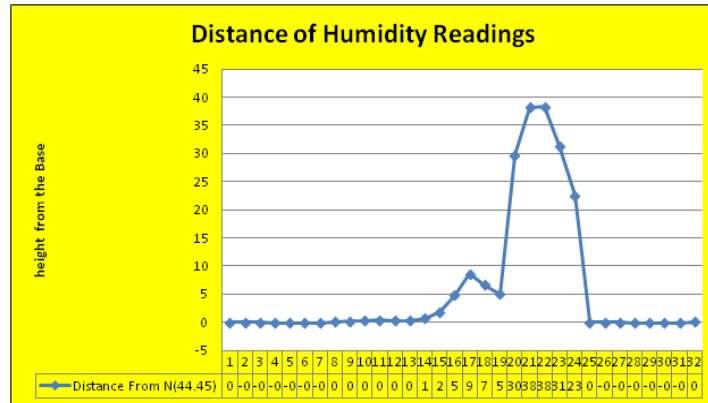


FIGURE 2.DISTANCE OF DATA ELEMENTS

TABLE 2. NODE SIGNAL VALUES USING DVD ALGORITHM

First Ten	Second Ten	Third Ten
44.45	44.85	82.61
44.42	44.78	82.79
44.42	44.71	75.74
44.38	45.18	66.97
44.35	46.26	44.45
44.32	49.26	44.42
44.38	53.06	44.42
44.52	51.12	44.38
44.65	49.48	44.35
44.71	74.17	44.32
Avg=44.46, Sum= 444.6 Highest=44.71 Trans=10	Avg=50.287 Sum= 502.87 Highest=74.17 Trans=10	Avg=57.445 Sum= 574.45 Highest=82.79 Trans=10

5.2 DVD Algorithm to Trace Outliers in Node Signal Values

The DVD Algorithm to Trace Outliers in Node Signal Values within a Specified Period is listed below. Let the Average of all the Node readings be NBaseValue. .

NBaseValue.= Average(Readings from node signal values)

Let the Upper Range in the Range be defined as NBaseValue. + 5% of NBaseValue.

Let the Lower Range in the Range be defined as NBaseValue. - 5% of NBaseValue.

The Record set D = Average(Readings), Count(Trans(in Node))

For i = 1 to N //Number of Records in D

NMaxSigVal = maximum (reading)

NMinSigVal = Minimum(Reading)

If (NMaxSigVal > UpperRange)

“Differential Value”

End if Cond.

If (NMinSigVal < LowerRange)

“Differential Value”

End if Cond.

End for (i)

The Values in Table 1 would be summed up by the DVD Algorithms as listed in Table 2

Table 3 and Figure 3 depict the node values with NN-DVD classifiers.

TABLE 3. NODE SIGNAL VALUES WITH NN-DVD CLASSIFIERS

Batches	Avg	Trns	Highest
Batch 1	44.46	10	44.71
Batch 2	50.287	10	74.17
Batch 3	57.445	10	82.79

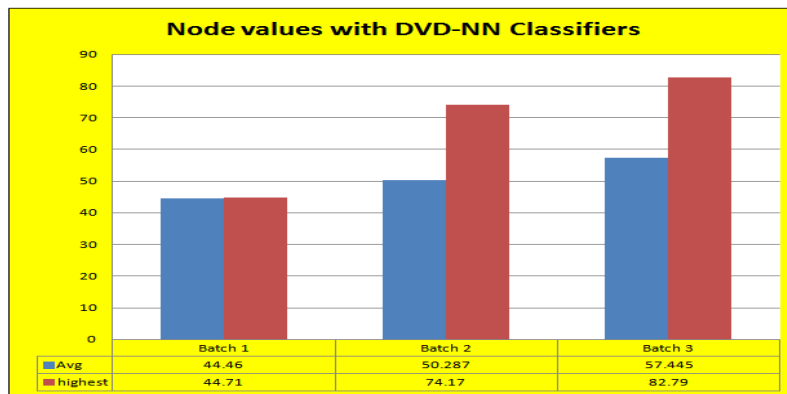


FIGURE 3. DISTANCES BASED ON AVERAGE AND HIGH VALUES

The Distances based on Euclidean Distance formula is listed in (1)

$$D(X, Y) = \sum_{i=1}^n (X_i - Y_i)^2 \tag{1}$$

The Values are Commonly Divided by the Sum Amount to keep the Calculation Simpler using the formula. The classified values would translate to Table 4.

TABLE 4. EUCLIDEAN DISTANCES BETWEEN THE SAMPLES

Batches	Avg	Euclidean Value	highest	Euclidean Value
Batch 1	44.46	=(44.46/444.6)	44.71	=(44.71/444.6)
Batch 2	50.287	=(50.287/502.87)	74.17	=(74.17/502.87)
Batch 3	57.445	=(57.445/574.45)	82.79	=(82.79/574.45)

Node Signal Value with DVD would be result in a graph of Outliers which is clear on the outliers. The resulting graph will be more pronounced and is depicted in Figure 4.

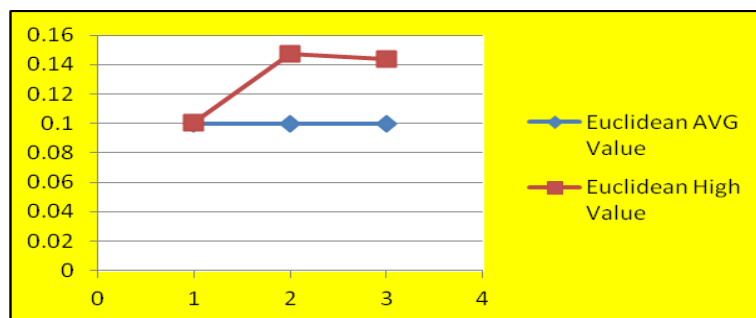


FIGURE 4. OUTLIERS IDENTIFIED WITH DVD

6. Conclusions

WSNs have become an integral part of major network based applications. Moreover, current trend in IT like IOT use WSN many ways. WSN can meet application demands of timely information. The internet and WSNs are being used by more and more businesses. WSN data has to accurate and perfect, specifically in mission critical applications and decision support system. Abnormalities can occur at any point in WSN information capture and transmissions. Anomalies cannot be ignored as they contribute incorrect summations or analysis of data. This paper has presented a new algorithm based on NN for identifying abnormalities in WSNs. DVD is easily implementable and can used to identify outliers even in large data sets. The DVD algorithm can also be implemented in any application, where outliers or differential values can hamper effective decision making based on available information. This paper has also demonstrated the effectiveness of the proposed algorithm with an example of WSN node readings. It can be concluded that DVD is simple, efficient and can be applied to any domain of WSN, where there are possibilities of anomalies or outliers or differential values.

REFERENCES

- [1] Zhang, Y.; Meratnia, N.; Havinga, P. Outlier detection techniques for wireless sensor networks: A survey. *IEEE Commun. Surv. Tutor.* 2010, 12, 159–170
- [2] Akyildiz, I.F.; Su, W.; Sankarasubramaniam, Y.; Cayirci, E. *Wireless sensor networks: A survey.* *Comput. Netw.* 2002, 38, 393–422.
- [3] Chandola, V.; Banerjee, A.; Kumar, V. Anomaly detection: A survey. *ACM Comput. Surv.* 2009, 41, 15..
- [4] Bettencourt, S.M.A.; Hagberg, A.A.; Larkey, L.B. Separating the Wheat from the Chaff: Practical Anomaly Detection Schemes in Ecological Applications of Distributed Sensor Networks. In *Proceedings of the 3rd IEEE International Conference on Distributed Computing in Sensor Systems, Santa Fe, NM, USA, 18–20 June 2007*; pp. 223–239..
- [5] Zhang, Y.; Meratnia, N.; Havinga, P. Adaptive and Online OneClass Support Vector Machine-Based Outlier Detection Techniques for Wireless Sensor Networks. In *Proceedings of the International Conference on Advanced Information Networking and Applications Workshops, Bradford, UK, 26–29 May 2009*; pp. 990–995 Kossinets, Gueorgi, and Duncan J. Watts. "Origins of Homophily in an Evolving Social Network." *American Journal of Sociology* 115 (2009): 405–50. Accessed February 28, 2010. doi:10.1086/599247.
- [6] Meratnia, N.; Zhang, N.; Havinga, P.J. Ensuring high sensor data quality through use of online outlier detection techniques. *Int. J. Sens. Netw.* 2010, 7, 141–151.
- [7] Siripanadorn, S.; Hattagam, W.; Teaumroog, N. Anomaly detection in wireless sensor networks using self-organizing map and wavelets. *Int. J. Commun.* 2010, 4, 74–83..
- [8] Shahid, N.; Naqvi, I.; Qaisar, S. Real Time Energy Efficient Approach to Outlier & Event Detection in Wireless Sensor Networks. In *Proceedings of the IEEE International Conference on Communication Systems (ICCS), Singapore, 21–23 November 2012*; pp. 162–166.
- [9] N. Beckmann, H. P. Kriegel, R. Schneider, and B. Seeger. The Rtree: an efficient and robust access method for points and rectangles. *ISIGMOD*, 1990.
- [10] M. Bawa, T. Condie, and P. Ganesan. Lsh forest: self-tuning indexes for similarity search. In *WWW*, 2005.
- [11] Kamal Malik and H.Sadawarti, Comparative Analysis of Outlier Detection Techniques, *International Journal of Computer Applications*, Volume 97– No.8, July 2014.
- [12] C. Böhm and F. Krebs. The k-nearest neighbor join: Turbo charging the kdd process. *Knowl. Inf. Syst.*, 6(6):728–749, 2004.
- [13] T. M. Chan. Approximate nearest neighbor queries revisited. In *SoCG*, 1997.
- [14] R. Fagin, R. Kumar, and D. Sivakumar. Efficient similarity search and classification via rank aggregation. In *SIGMOD*, 2003.



Dr. Usha Dhanabal, M.C.A., M.Phil., M.Tech., Ph. D (CS & IT) is currently working as an Assistant Professor in the Department of Computer Science at Mother Teresa Womens's University, Kodaikanal, Tamilnadu, India. Since 2002.,she has 11 years of Teaching and Research experience. Prior to joining the university, she worked as an Assistant Professor at National Engineering College of Kovilpatti, Tamilnadu, India for six years and she also worked at Infant Jesus College of Engineering Tirunelveli, Tamilnadu, India for three years. She received her M.Tech & Ph. D in Computer Science & Information Techonology from M.S University, Tirunelveli Tamilnadu, India . Her area of interest are Networking and Wireless Sensor Networks. Most of the research work has been on design, understanding and performance of Wireless Sensor Networks. She has also authored many International Journal publications of IJCA, IJCCIS, IJSER and IJCSEITR.